# Temperature-dependent Gain and Loss in Room-temperature Continuous-wave Quantum Cascade Lasers between 8.2-10.3µm

Zhijun Liu, Claire F. Gmachl, Liwei Cheng, Fow-Sen Choa, Fred J. Towner, Xiaojun Wang, and Jenyu Fan

***Abstract*—Temperature-dependent optical gain and waveguide loss have been measured for room temperature, continuous-wave Quantum Cascade Lasers at λ ~ 8.2, 9.6 and 10.3 µm using the Hakki-Paoli method. The results confirm that the gain coefficient decreases with increasing temperature, while the waveguide loss increases or decreases with temperature with the trend depending on the individual laser design.**

***Index Terms*—Optical gain, waveguide loss, midinfrared, quantum cascade (QC) laser.**

## I. Introduction

QUANTUM cascade (QC) lasers are of particular interest for trace gas sensing applications since their wavelengths can be designed anywhere in the midinfrared, which contains the strong fingerprint absorption features of many gaseous pollutants and some human-disease related gases. Owing to improved laser design, material growth and device packaging, the performance of QC lasers has improved significantly, and high power, room-temperature, continuous-wave (CW) operation has been demonstrated repeatedly [1-4]. Optical gain and waveguide loss are two important parameters in the understanding of QC laser performance and in improving laser designs to achieve even better performance. However, the data regarding these two parameters are very limited in the current literature for high performance QC lasers, and with the waveguide loss being reported only at room temperature in some cases [3]. Here, by using the Hakki-Paoli method [5], we measured the optical gain and waveguide loss at different temperatures on room temperature, CW QC lasers at λ~8.2, 9.6 and 10.3 µm. Besides confirming the expectation for the temperature dependence of the gain coefficient, our results indicate a temperature-dependent waveguide loss that depends on the individual laser design, and which can be attributed to a combination of free carrier absorption and spurious resonant intersubband absorption.

Manuscript received March 14, 2007. This work was in part supported by DARPA L-PAS and MIRTHE (NSF-ERC).

Z. Liu and C. F. Gmachl are with the Department of Electrical Engineering and the Princeton Institute for the Science and Technology of Materials, Princeton University, Princeton, NJ 08544 USA (e-mail: zhijunl@princeton.edu).

L. Cheng and F.-S. Choa are with the Department of Computer Science and Electrical Engineering, University of Maryland, Baltimore, MD 21250 USA.

F. J. Towner is with Maxion Technologies Inc., Hyattsville, MD 20782, USA

X. Wang and J. Fan are with AdTech Optics, City of Industry, CA 91748, USA

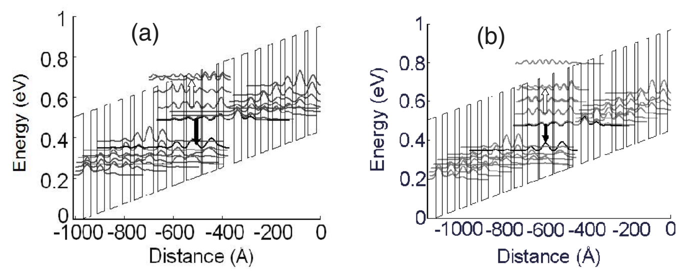


Fig. 1 Conduction band diagram of a portion of the active regions and injectors and the moduli squared of the relevant wave functions of a ~9.6µm (a) and ~10.3µm (b) QC lasers with a 4 quantum well active region. An electric field of 45 and 39 kV/cm is applied in (a) and (b), respectively. The solid arrows indicate the laser transitions. The open arrows represent pathways of resonant absorption

## II. Experiment

The QC lasers in this study were designed as "two phonon resonance" QC lasers [6]. The 8.2µm QC laser structure and its device performance have been described in ref. [4]. For the 9.6um and 10.3µm QC lasers, their electron energy band diagrams are shown in Fig.1 (a) and (b), respectively. The layer sequence (in Å) of one period of active region and injector is **42**/20/**7**/58/**9**/59/**9**/49/**24**/35/**15**/34/**14**/33/**16**/32/**19**/31/**23**/30/**25**/30 for the 9.6µm QC laser and **40**/19/**7**/65/**9**/63/**9**/54/**24**/38/**18**/37/**17**/37/**17**/37/**17**/36/**19**/35/**23**/34/**27**/33 for the 10.3µm QC laser, where $In_{0.52}Al_{0.48}As$ barrier layers are in bold, $In_{0.53}Ga_{0.47}As$ well layers are in roman, and the n-doped ($1\times10^{17}$ $cm^{-3}$) layers are underlined. The 9.6µm QC lasers have been processed into deep-etched, metal-clad ridge waveguide. The 10.3µm QC lasers have been processed into both ridge waveguide and buried heterostructure lasers. With a 3.5mm long cavity and high reflectivity coating on the back facet, these lasers operate in CW up to room temperature. However, the lasing thresholds of these QC lasers are still much higher than the designed values. To get a better understanding of this difference, we used the Hakki-Paoli method to determine the gain and waveguide loss in 1.5mm long devices. The high resolution subthreshold amplified spontaneous emission spectra were recorded with a Magna 860 Fourier Transform Infrared Spectrometer (FTIR) under conditions of 200 scans and 0.125cm$^{-1}$ resolution. The spectra were measured at different heat sink temperatures. A typical spectrum is shown in the inset of Fig. 2 (a).

## III. Results and Discussions

The extracted gain coefficient and waveguide loss are shown in Fig. 2 (a), (b), and (c) for the 8.2, 9.6, and 10.3μm QC lasers, respectively. The gain coefficient decreases monotonously with increasing temperatures for all lasers. This is understandable from the effects of decreasing scattering lifetimes, broadening of the gain linewidth, and thermal-backfilling at higher temperature. The measured gain coefficients agree well with the theoretical values for the 8.2μm QC laser, and are slightly lower than the theoretical values for the 10.3μm QC lasers. The waveguide loss for all lasers is two times higher than theoretical estimation from the free carrier absorption (5-6.6cm$^{-1}$). Also, as the temperature increases, it remains nearly unchanged for the 9.6μm QC lasers, but increases for the 8.2μm QC laser, and decreases first and then increases for the 10.3μm QC lasers. In addition, for the 10.3μm QC lasers, the buried heterostructure laser has nearly the same gain coefficient, but a lower waveguide loss as compared with the ridge waveguide laser. Nevertheless, the general shapes of the temperature dependence are identical for both lasers, indicating an origin in the active laser core rather than the external waveguide. These temperature-dependent, relatively high waveguide losses suggest some loss mechanisms other than free-carrier absorption. Resonant absorptions were found and indicated by open arrows in Fig.1. Their absorptions are estimated as 1.69, 1.71, and 1.72 cm$^{-1}$. Though this can't fully account for the extra loss, the resonant absorptions and free carrier loss can explain the temperature-dependent behavior of the waveguide loss qualitatively. As temperature increases, the free carrier absorption increases due to decreasing electron mobility. Meanwhile, the resonant absorption levels are shifted either closer to or farther away from resonance resulting in both as increasing or decreasing waveguide loss with temperature. The free carrier loss together with resonant absorption can result in the temperature-dependence of waveguide loss observed in the experiments.

## IV. Summary

Using the Hakki-Paoli method, we have measured the optical gain and waveguide loss of high temperature CW QC lasers at λ~8.2, 9.6 and 10.3μm at different temperatures. The results confirm that the gain coefficient decreases with increasing temperatures, while the waveguide loss varies with temperature with the trend depending on the actual laser active region designs, which is also supported by band structure calculation. This suggests additional loss from resonant intersubband absorption.

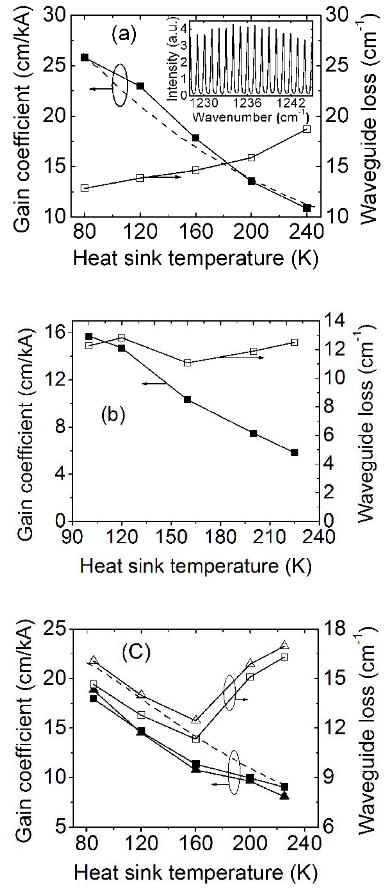


Fig. 2 Gain coefficient (solid symbols) and waveguide loss (open symbols) obtained from the Hakki-Paoli method at different heat sink temperatures for: (a) a 1.5mm long, 9μm wide ridge waveguide QC laser at λ~8.2μm. The dashed line is the theoretical gain coefficient. The inset shows part of a typical amplified spontaneous emission spectrum at 160K; (b) a 1.5mm long, 15μm wide ridge waveguide QC laser at λ~9.6μm; (c) a 1.5mm long, 16μm wide, ridge waveguide QC laser (triangles) and a buried heterostructure QC laser (squares) at λ~10.3μm. All devices are operated in CW mode. Lines are guides to the eye.

## Acknowledgment

This work was in part supported by DARPA L-PAS and MIRTHE (NSF-ERC).

## References

[1] M. Beck, et al., "Continuous wave operation of a mid-infrared semiconductor laser at room temperature," Science **295**, 301-305 (2002).

[2] J. S. Yu, et al., "Temperature dependent characteristics of λ~3.8μm room-temperature continuous-wave quantum-cascade lasers," Appl. Phys. Lett. **88**, 251118-1-251118-3 (2006).

[3] L. Diehl, et al., "High-power quantum cascade lasers grown by low-pressure metal organic vapor-phase epitaxy operating in continuous wave above 400 K," Appl. Phys. Lett. **88**, 201115-1-201115-3 (2006).

[4] Z. Liu, et al., "Room-temperature continuous-wave quantum cascade lasers grown by MOCVD without lateral regrowth," IEEE Photon. Technol. Lett. **18**, 1347-1349 (2006).

[5] B. W. Hakki, et al., "Gain spectra in GaAs double-heterostructure injection lasers," J. Appl. Phys. **46**, 1299–1306 (1975).

[6] D. Hofstetter, et al., "Continuous wave operation of a 9.3μm quantum cascade laser on a Peltier cooler," Appl. Phys. Lett. **78**, 1964-1966 (2001).